Density Functional Theory Analysis of Benzene (De)hydrogenation on Pt(111): Addition and Removal of the First Two H-Atoms

Mark Saeys,[†] Marie-Françoise Reyniers,[†] Matthew Neurock,[‡] and Guy B. Marin*[,†]

Laboratorium voor Petrochemische Techniek, Universiteit Gent, Krijgslaan 281 S5, B-9000 Gent, Belgium, and Department of Chemical Engineering, School of Engineering and Applied Science, University of Virginia, Thornton Hall, Charlottesville, Virginia 22904-4741

Received: September 27, 2002; In Final Form: January 15, 2003

The hydrogenation and dehydrogenation of benzene on Pt(111) is examined from first principles using DFT-GGA cluster calculations. The reactive benzene species is adsorbed at the hollow site. The addition of the first H-atom has a barrier of 74 kJ/mol and is +11 kJ/mol endothermic. There are five different pathways available for the addition of the second hydrogen atom. The dominant path is the one that forms the 1,3-dihydrobenzene intermediate. This reaction has a barrier of 72 kJ/mol and is +34 kJ/mol endothermic. The hydrogenation of the $C_6H_7^*$ intermediate can also form 1,3-cyclohexadiene, which has a barrier of 91 kJ/mol and is +38 kJ/mol endothermic, or 1,4-cyclohexadiene, which has a barrier of 115 kJ/mol and is +36 kJ/mol endothermic. Two types of hydrogenation mechanisms were distinguished. The "three-centered" mechanism was found to be more favorable than the "slip" mechanism. The dehydrogenation of benzene to phenyl is +76 kJ/mol endothermic. Therefore benzene dehydrogenation is neither thermodynamically nor kinetically a favorable reaction path. Dehydrogenation to *o*-benzyne is +14 kJ/mol endothermic relative to benzene. The calculated barriers are in qualitative and quantitative agreement with experimental data.

1. Introduction

The catalytic hydrogenation and dehydrogenation of cyclic molecules are important reactions in the efficient production of fuels.[1,2] The catalytic dehydrogenation of cyclic alkanes and alkenes to aromatic hydrocarbons is one of the key paths to gasoline during the reforming process.[3] Catalytic reforming is responsible for the upgrading of over 11 million barrels of oil a day worldwide.[4] During reforming, relatively large aliphatic molecules with low octane numbers are converted into hydrocarbons having higher octane numbers via a complex network of isomerization, hydrogenation, dehydrogenation, and hydrodrocyclization steps.

Hydrocracking is another major petrochemical process. Here, heavy hydrocarbons, with high concentrations of aromatic components, are converted to smaller, branched hydrocarbons under a high pressure of hydrogen over bifunctional transition metal/zeolite catalysts. The major products are high-value hydrocarbons in the kerosene and diesel boiling range. During the hydrocracking of hydrocarbons, hydrogenation is an important step. Recent environmental legislation has placed stringent limits on the concentration of benzene and other aromatics present in fuels.[5,6] Also, the removal of aromatics increases the quality of a diesel fuel.[6] For these reasons, the hydrogenation of aromatic hydrocarbons is of increasing interest. Under typical process conditions, the metal-catalyzed hydrogenation reactions for alkenes are in quasi-equilibrium. The hydrogenation of aromatic hydrocarbons is more difficult and hence quasi-equilibrium cannot be assumed a priori.

The hydrogenation of benzene to cyclohexane is also an important step in the industrial production of nylon(66).[7]

A detailed knowledge of the elementary steps of the hydrogenation and dehydrogenation mechanism will ultimately aid in optimizing these different industrial processes.

The hydrogenation of aromatic hydrocarbons as well as the dehydrogenation of cyclic alkanes and alkenes has received much attention. Classical kinetic studies have been performed for the hydrogenation of benzene,[8−30] toluene,[20,31−36] and other aromatic hydrocarbons,[37−42] yielding an array of different kinetic models and postulated mechanisms.

Surface science studies have been performed on well-defined Pt(111) for the chemisorption and dehydrogenation of cyclohexane,[43−53] cyclohexene,[51−58] cyclohexadiene,[51−53,58−61] benzene,[50,62−66] and phenyl.[67] Reaction intermediates have been identified and experimental values for some of the associated activation barriers have been reported. This work has recently been discussed in detail by Koel et al.[68]

Also, some theoretical studies have addressed the adsorption and hydrogenation/dehydrogenation of cyclic hydrocarbons. Kang and Anderson[69] used semiempirical calculations to study cyclohexane adsorption and partial dehydrogenation. Benzene adsorption on model Pt(111) surfaces was examined with extended Hückel theory,[70] with density functional theory (DFT) with clusters of one and two Pt-atoms,[71−73] and with an ab initio third-order algebraic-diagrammatic-construction Green function method.[74] Recently, we used a reasonably large 22-atom cluster and fully periodic slab DFT calculations to study benzene[75] and 1,4-cyclohexadiene[76] chemisorption on Pt(111). Periodic slab DFT calculations have also been carried out for benzene adsorption on different Ni surfaces[77,78] on Ru(0001)[79] and on Al(111).[80] Ab initio cluster model calculations were carried out to analyze the adsorption of benzene on Cu and Pd.[81] Extended Hückel theory has been used to study the adsorption and dehydrogenation of cyclic C_5 hydrocarbons on Pt(111).[82,83]

* Corresponding author. E-mail address: Guy.Marin@rug.ac.be. Fax: ++32 9 2644999. Tel: ++32 9 2644516.
[†] Universiteit Gent.
[‡] University of Virginia.

10.1021/jp022166n CCC: $25.00
Published on Web 04/02/2003

Despite this wealth of experimental and theoretical studies little is known about the mechanism of benzene hydrogenation or cyclohexadiene dehydrogenation over Pt(111). First principle studies of hydrocarbon hydrogenation and dehydrogenation have been limited to molecules having a rather simple mechanism, such as methane,[84−86] and ethene.[87] One of the largest species examined has been maleic anhydride.[88]

For present day first principle calculations, benzene is a rather large molecule and therefore requires rather larger platinum clusters or unit cells. Moreover, benzene can be hydrogenated at six different positions, which leads to a complicated mechanism. Although the general reaction path is thought to follow the classical Horiuti−Polanyi mechanism[89] whereby hydrogen atoms add sequentially, little is known about the specific transformations.

In this paper, the addition of the first and the second hydrogen atoms to benzene will be discussed. In many kinetic studies, it is assumed that the addition of either the first or the second hydrogen atom is rate determining. Our results, however, indicate that this may not be the case. Second, we show that there is a preferred reaction path for the addition of the first and the second hydrogen atom; i.e., the hydrogen atoms do not add at random to the different carbon atoms. Finally, we compare our proposed mechanism and calculated activation barriers with experimental observations to help elucidate the experimental data.

In a number of kinetic models for the hydrogenation of aromatic molecules, dehydrogenated species are assumed to be the most abundant surface intermediates. This is similar to the model initially proposed by Farkas and Farkas[90] for ethene hydrogenation. In this paper the dehydrogenation of benzene is therefore studied up to benzyne. It will be shown that thermodynamically the dehydrogenation is not a favored pathway.

2. Computational Approach

2.1. Methods. All calculations were carried out using density functional theoretical methods and performed using the Amsterdam Density Functional (ADF2000) package.[91] Generalized gradient (GGA) corrections to the Vosko−Wilk−Nusair[92] local density (LDA) exchange-correlation energy were carried out self-consistent using the Becke−Perdew (BP86)[93,94] functionals. Scalar relativistic effects were included through the Zero-Order Regular Approximation (ZORA[95]) Hamiltonian. Basis sets were of double-ζ quality and constructed from Slater Type Orbitals (STO). The innermost atomic shells were kept frozen and replaced by a fully relativistic core potential. The cores were frozen up to and including the Pt 4f and the C 1s shell. Decreasing the Pt frozen core to the 4d shell, and thus allowing more electrons to participate in bond formation, increases the calculated adsorption energy by less than 5 kJ/mol. Unrestricted DFT calculations were used for all the calculations reported herein where the spin multiplicity was optimized to find the lowest energy spin states. ADF standard self-consistent field (SCF)-convergence and geometry-convergence criteria were applied.[91] Tightening these criteria changed the calculated energy by less than 0.1 kJ/mol. The numerical precision parameter was set at $10^{-5.0}$. Symmetry was exploited whenever possible, which increased the computational efficiency significantly. The Pt(111) surface was modeled using a two-layered Pt_{22} cluster with 14 atoms in the top layer. The Pt−Pt distance was kept fixed at the bulk value of 277 pm.[96] Adsorption and reaction were studied on the central atoms of this cluster. This approach was shown to yield reasonably accurate adsorption energies for benzene,[75] 1,4-cyclohexadiene,[76] and cyclohexene adsorption on Pt(111) in comparison with fully periodic slab calculations in which the surface layers were allowed to relax, and with known experimental data.

Transition states were isolated by performing a series of calculations to map out a portion of the potential energy surface. We start by examining a series of structures along the linear transient between the reactant and product states. The reaction path involves the breaking of M−C and M−H bonds and the formation of a C−H bond. A series of states that lie at 10 pm increments along the linear path between the reactant and product state are chosen as starting structures to examine the potential energy surface. The C−H distance is constrained at each of these steps, but all of the other modes are allowed to be optimized. This leads to a first-order approximation of the transition state geometry. This initial guess was then used as input to a more rigorous mode following search strategy to isolate a true transition state. In this type of calculation an approximate Hessian is evaluated iteratively. It was verified that this Hessian has one and only one negative eigenvalue. Then the path from the transition state to the products and to the reactants is traced, using the Intrinsic Reaction Coordinate method.[97] All these calculation were performed on smaller constrained clusters containing 5−10 Pt atoms. The optimized transition state is then used as an initial guess in a transition state optimization on the large Pt_{22} cluster. Also here it was verified that the approximate Hessian of the final geometry has exactly one negative eigenvalue.

Gas-phase enthalpies of formation were calculated with Gaussian98[98] with the BP86/cc-pVTZ DFT method as well, and in some cases also with the post-HF CBS-QB3[99] method. Frequency calculations for the double-ζ basis set where done with BP86/cc-pVDZ level.

Chemisorption energies were computed by subtracting the energy of the optimized gas-phase adsorbate and the platinum cluster from the energy of the optimized adsorbate-cluster complex.

$$\Delta E_{\text{ads}} = E_{\text{adsorbate/metal}} - E_{\text{adsorbate}} - E_{\text{metal}} \qquad (1)$$

The energy of reaction was computed by subtracting the chemisorption energies for the products and the reactants from the gas-phase energy of reaction. In this way the two reactant species are assumed to be noninteracting in the reactant state.

$$\Delta E_{\text{r}}(\text{surface}) = \Delta E_{\text{r}}(\text{gas phase}) + \Sigma\Delta E_{\text{ads,products}} - \Sigma\Delta E_{\text{ads,reactants}} \qquad (2)$$

2.2. Influence of Thermal Corrections. To test the theoretical methods, gas-phase thermochemical data were calculated and compared with experimental values. Ab initio enthalpies of formation are generally derived by combining calculated atomization enthalpies with experimental enthalpies of formation of the atoms.[100] This approach is very susceptible to computational and experimental errors on the atomic species. Therefore in this work, gas-phase *reaction* enthalpies and energies were calculated for (de)hydrogenation reactions of the form:

$$^{x}/_{2}H_2 + C_6H_6 \rightarrow C_6H_{6+x} \qquad (3)$$

$$C_6H_6 \rightarrow C_6H_{6-x} + {}^{x}/_{2}H_2 \qquad (4)$$

i.e., relative to the enthalpies of formation of benzene and dihydrogen. For most of the molecules pertinent to our study

TABLE 1: Influence of Corrections on Enthalpy of Reaction

	H	benzene	cyclohexadienyl
E_{elec}[a]	0	0	−126.5
zero point energy[b]	0	255.8	276.3
$E_{trans,vib,rot}(0\rightarrow 298\ K)$[b]	6.2	14.4	16.2

[a] Calculated with ADF BP86/DZ. [b] Calculated with Gaussian98 BP86/cc-pVDZ.

accurate experimental gas-phase enthalpies of formation are available. To obtain accurate $\Delta_f H°$ (298 K) for species for which no accurate experimental data are available, the CBS-QB3 ab initio method was applied. In a separate study,[101] it was found that heats of formation for a training set of 58 hydrocarbon molecules and radicals could be calculated with a mean absolute deviation of 2.5 kJ/mol with the CBS-QB3 method. In our approach,[101] enthalpies of formation are obtained by combining calculated atomization enthalpies with fine-tuned enthalpies of formation for the C and H atom, to minimize systematic error. For H a "fine-tuned" enthalpy of formation of 217.7 kJ/mol is used, where the experimental value is 218.0 kJ/mol,[102] and for C a "fine-tuned" enthalpy of formation of 715.4 kJ/mol is used, where the experimental value is 716.7 kJ/mol.[102] Stated differently, a systematic correction of −0.3 kJ/mol is used per hydrogen atom and −1.3 kJ/mol per carbon atom.

In an ab initio calculation the reaction enthalpy is computed in three parts (5). From the SCF calculations the electronic energy difference, ΔE_{elec}, is obtained. The zero-point vibrational energy, ΔE_{ZPE}, and the internal energies due to translation, vibrational motion and rotational motion, $\Delta E_{vib,trans,rot}(0\rightarrow 298\ K)$ K), are obtained from frequency calculations and statistical thermodynamics.[103]

$$\Delta H^0_r(298\ K) = \Delta E_{elec,r} + \Delta E_{ZPE} + \Delta E_{vib,trans,rot}(0\rightarrow 298\ K)$$

$$\Delta E_{ZPE} = \sum_{i=1}^{N} {}^1/_2 h\nu_i = \sum_{i=1}^{N} 5.985 \frac{\text{J·cm}}{\text{mol}} \omega_i \qquad (5)$$

where ν_i is the vibrational frequency in s^{-1} and ω_i is the vibrational wavenumber in cm^{-1}.

In a hydrogenation reaction, a new hydrogen−carbon bond is formed. In this reaction the H-atom loses its translational internal energy, but three additional vibrational modes originate in the product, leading to an increase of the zero point vibrational energy (ZPE). In Table 1 the three contributions are summarized for H addition to benzene. It can be seen that the change in ZPE decreases the exothermicity of the reaction by 21 kJ/mol. The three additional vibrations have frequencies of 1123, 1350, and 2850 cm^{-1} and thus give rise to an increase of the ZPE by +32 kJ/mol (eq 5). Also other vibrational frequencies are shifted during the course of the reaction, leading to +21 kJ/mol. The change in internal energies due to translation, vibrational and rotational motion decreases the exothermicity slightly by 4.4 kJ/mol. It is therefore important to include all terms of eq 5 to calculate the reaction enthalpy.

Table 2 lists the ab initio reaction electronic energies and the reaction enthalpies at two different levels of theory along with the experimental ΔH^0_r(298 K). The $\Delta E_{elec,r}$ with BP86/DZ deviate substantially from the experimental data. As is obvious from the previous paragraph, the main source is the neglect of ΔE_{ZPE} and $\Delta E_{vib,trans,rot}(0\rightarrow 298\ K)$. Inclusion of the two terms brings the calculated reaction enthalpies (third column of Table 2) in better agreement with experimental data. The mean absolute deviation (MAD) between theory and experiment is 12.3 kJ/mol. Increasing the basis set to cc-pVTZ does not improve the agreement, in fact the MAD increases to 14.0 kJ/mol, although the required CPU-time increases 10-fold.

TABLE 2: Gas-Phase Enthalpies of (De)Hydrogenation (kJ/mol) for the Various Reaction Intermediates, Starting from Benzene and Hydrogen (Reactions 3 and 4)

species	$\Delta E_{elec,r}$ BP86/DZ	ΔH^{ϕ}_r BP86/DZ	ΔH^{ϕ}_r BP86/cc-pVTZ	ΔH^{ϕ}_r exptl
cyclohexadienyl	104.2	109.4	118.9	121.3[a]
1,3-CHD	−3.7	18.4	41.2	27.5[a]
1,4-CHD	0.7	22.3	41.9	28.0[a]
1,3-dihydrobenzene	202.1	213.1	231.8	242.0[a]
H-atom	230.7	219.8	222.4	218.0[b]
CHA	−296.4	−219.9	−167.0	−206.0[b]
phenyl	265.4	248.7	241.3	261.3[a]
benzyne	423.0	392.5	369.8	378.0[a]

[a] Calculated with CBS-QB3. [b] Reference 102.

TABLE 3: Calculated Enthalpies and Electronic Energies of Adsorption (kJ/mol)

species	$\Delta E_{elec,ads}$	ΔH_{ads}(298 K)
benzene-hollow	−71	−69
benzene-bridge	−102	−104
1,4-cyclohexadiene	−145	−144

To test the influence of the ZPE and the internal energy due to translation, vibrational and rotational motion on the calculated adsorption *enthalpies*, $\Delta E_{elec,ads}$ and ΔH_{ads}(298 K) were calculated for 1,4-cyclohexadiene adsorption and for benzene adsorption at two different sites (Table 3). The difference between the adsorption energies and enthalpies is less than 2 kJ/mol. The reason is that the newly formed C−Pt bonds have very low vibrational frequencies and thus contribute little ZPE to the adsorption enthalpy (eq 5). Therefore, for molecular adsorption, it is a good approximation to neglect thermal corrections.

For the calculation of adsorption enthalpy in the case of *dissociative* adsorption, e.g., dihydrogen adsorption, the experimental gas-phase enthalpy of formation of the hydrogen atom, and the binding energy of the hydrogen atom to the Pt-surface have to be combined. The loss of ZPE upon H_2 adsorption is thus calculated from the ZPE of the dihydrogen molecule. If the loss of ZPE is neglected, the heat of dihydrogen adsorption is underestimated by 26 kJ/mol.

The discussion in the previous paragraphs leads to a method to improve the calculated enthalpy diagram for benzene hydrogenation. Instead of using the calculated electronic energies of the adsorbed species, we start from experimental gas-phase enthalpies for the different intermediates. The gas-phase *enthalpy* diagram is then combined with the calculated adsorption *energies* for the different intermediates (as in eq 2). This leads to the enthalpy diagram for the adsorbed intermediates. This approach cannot be used, however, for the activation energies, because experimental gas-phase enthalpies for the transition states do not exist. The calculation of the ZPE and the internal energy for the transition state (on the metal cluster) is computationally very demanding and beyond our CPU resources. Instead we use theory to obtain upper and lower limits to the calculated activation barriers. During the hydrogenation reaction a C−H bond is formed. This increases the ZPE, making the reaction less exothermic (Figure 1). If we use the calculated (electronic) hydrogenation activation energy, it is implicitly assumed that the ZPE does not change in going from the reactants to the transition state. To have thermodynamic consistency, the dehydrogenation activation energy is then obtained from the reaction enthalpy (which includes the ΔZPE and the $\Delta E_{vib,trans,rot}(0\rightarrow 298\ K)$) (Figure 1). If we use the calculated (electronic) dehydrogenation activation energy and

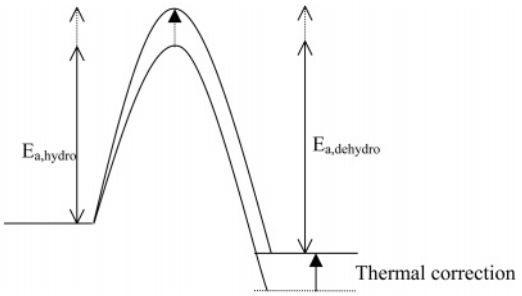

Figure 1. Illustration of the possible ways to calculate the activation energy.

calculate the hydrogenation activation energy from the reaction enthalpy, it is implicitly assumed that the ZPE of the transition state is the same as in the hydrogenated product. In this paper we will therefore report two values for the activation energy. For the hydrogenation, the low value corresponds to the ab initio calculated barrier, i.e., without ZPE.

In the transition state, the stretch frequency associated with the forming C−H bond is the reaction coordinate and thus does not contribute to the ZPE. Therefore, the ZPE increase from the reactant to the transition state is expected to be less than the increase from the transition state to the hydrogenated product. Therefore, we believe the lower value for the hydrogenation barrier is closer to the reality than the higher value.

3. Results

3.1. Benzene Adsorption. In a previous paper[75] we examined benzene adsorption over Pt(111) using cluster as well as periodic slab density functional theory calculations. Benzene can adsorb at different high-symmetry sites of the (111) surface. The preferred adsorption site was found to be the bridge(30) site (Figure 2), with a calculated adsorption enthalpy of −102 kJ/mol. A second important site is the hollow(0) site (Figure 2) with a calculated adsorption energy of −71 kJ/mol. Adsorption at the hollow-hcp site was found to be 6 kJ/mol more stable than at the hollow-fcc site. In the following, we do not distinguish between the fcc and hcp site because their stability difference is so small.

Benzene molecules adsorbed at the hollow(30) and bridge(0) site were found to be transition states during the surface diffusion and relax to the bridge(30) and hollow(0) sites, respectively. The diffusion of the hollow-bound benzene was found to have a low activation barrier, because the difference in energy between the hollow(0) and bridge(0) site is only 10 kJ/mol. The diffusion of benzene from its more stable bridge(30) site is more activated, whereby the difference in energy between the bridge(30) and the hollow(30) site is about 50 kJ/mol. Adsorption of benzene at the top site is unfavorable.

To verify the accuracy of the cluster approach, computationally more demanding periodic DFT calculations were performed. The results showed that the adsorption energies at the bridge(30) and hollow(0) sites were −117 and −75 kJ/mol, respectively, which is in good agreement with the cluster results.[75]

TPD data[50,63] confirm that benzene adsorbs at two different sites. Comparison of frequency calculations with spectroscopic data from RAIRS[64] and HREELS[65] confirms that the spectrum observed at low benzene coverage corresponds with benzene adsorbed at the bridge(30) site. Both the calculated frequency and the relative intensities of the peaks are in good agreement with the experimental spectra.

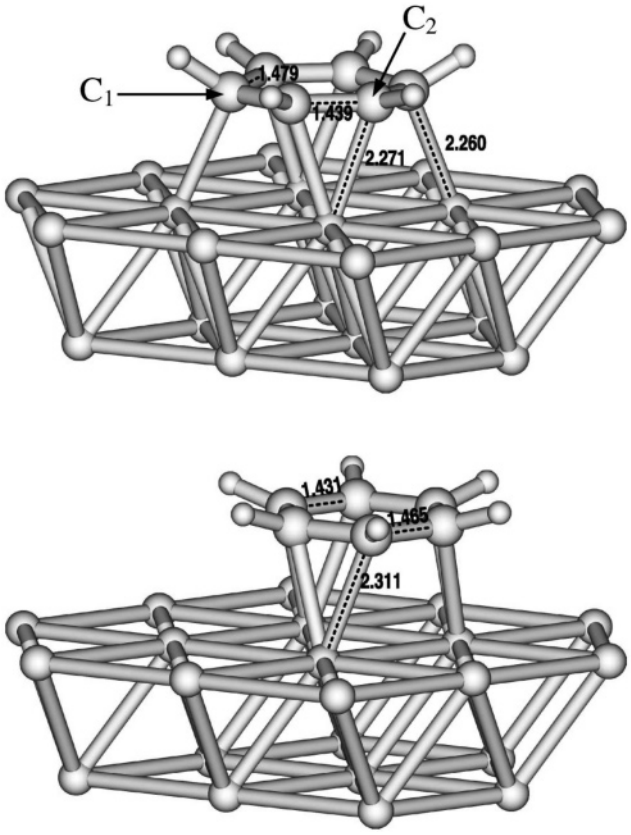

Figure 2. Benzene adsorbed at the bridge(30) (left) and the hollow(0) (right) site. Bond lengths are indicated in ångstroms.

The experimental spectra change with increasing coverage. The peaks that develop with increasing coverage correspond to the calculated spectrum for benzene adsorbed at the hollow site. Benzene adsorbed at the bridge site on Pt(111) directly interacts with 4 metal atoms whereas benzene adsorbed at the hollow site only interacts with 3 as is shown in Figure 2. At higher surface coverage, benzene preferentially adsorbs at the hollow sites because this reduces the greater lateral interactions that exist at the bridge sites due to higher occupation of metal sites.

3.2. Dihydrogen Adsorption. Several surface science (for a recent discussion see: Podkolzin et al.[104]) and theoretical studies[105−108] have addressed dihydrogen adsorption on Pt(111). It has been established theoretically[106] and experimentally that dissociative hydrogen adsorption on Pt(111) is not activated. At low coverage, adsorption enthalpies in the range of 60−90 kJ/mol have been reported. Differential enthalpy diagrams of hydrogen adsorption show that the adsorption enthalpy decreases significantly with increasing coverage due to repulsive interactions.[104] Surface science and most theoretical studies indicate that hydrogen atoms adsorb at the fcc hollow site. However, DFT studies indicate that the differences in adsorption energy for the different sites are quite small with differences of only 2 kJ/mol between the most stable and the least stable adsorption sites. As a consequence H-atom surface diffusion is very fast.[108]

Olsen et al.[107] performed periodic DFT calculation with the BP86 functional including scalar-relativistic effects with the ZORA Hamiltonian. The highest adsorption energy of −94 kJ/mol was found for the top site, for the hollow sites adsorption energies of −64 and −70 kJ/mol were calculated. The neglect of relativistic effects was found to change the site preference.

In our calculations, which are the cluster-analogues of the work of Olsen et al.,[107] adsorption at the top site is also preferred, with an adsorption energy of −94 kJ/mol. For the fcc hollow

site an adsorption energy of −85 kJ/mol was calculated. These results are in agreement with experimental values as well as with results from periodic DFT calculations.

3.3. Addition of the First Hydrogen Atom. The hydrogenation of bridge(30) and hollow(0) site adsorbed benzene was studied. If we consider only the symmetry of the first Pt layer, we can identify two types of carbon atoms for a bridge bound benzene species (Figure 2). We call these two types C_1 and C_2. They have distinct hydrogenation pathways. The six carbon atoms for benzene adsorbed at the hollow site, however, are all equivalent (again considering only the symmetry of the first layer of the Pt surface). We therefore only examined one hydrogenation path for benzene adsorbed at the hollow site. The reactants, transition states and products for the addition of the first hydrogen atom for the three reaction paths are shown in Figure 3, together with the activation energies and the enthalpies of reaction and some important bond distances.

We examine the bridge-bound benzene first. Although the C−Pt distance for the two types of C-atoms is not too different (Figure 2), the corresponding hydrogenation pathways are very different. The addition of the hydrogen atom to C_1 involves a two-step process. When the hydrogen atom approaches benzene, it begins to localize electron density at the Pt atom, to which C_1 is also bound, thus forming a relatively strong Pt−H bond. This weakens the C_1−Pt bond and eventually leads to the breaking of the C_1−Pt bond. The hydrogen atom inserts into the Pt−C bond in a classical reductive elimination step. The transition state is relatively early in the reaction channel in that the C_1−H bond distance is still rather long at 175 pm. The C_1−Pt bond is stretched from 225 to 259 pm. This geometry is very similar to the three-centered transition state calculated for hydrogenation of di-σ-bound ethene on Pd(111)[87] as well as other substituted ethylene intermediates.[109]

Following the reaction path downhill, however, does not lead to cyclohexadienyl, but to an intermediate state with a tilted benzene molecule and an atop adsorbed hydrogen atom. The C_1−H distance in the intermediate state is quite large, indicative of a small C−H interaction. The H−Pt distance in the intermediate is equal to the distance found for H-adsorption. In the second step the benzene molecule tilts down to pick up the hydrogen atom. In the transition state the C_1−H distance is 157 pm, a typical value for a hydrogenation reaction.

The product cyclohexadienyl species has a long axial C−H bond of 111.5 pm. From a closer look at the different molecular orbitals of adsorbed cyclohexadienyl, it is found that through-bond interaction of the π-orbitals with the axial σ C−H bond in combination with strong electron donation from the axial σCH orbital to the surface is responsible for the weakening of the axial C−H bond. A similar effect was observed for adsorbed 1,4-cyclohexadiene.[76] For 1,4-cyclohexadiene this effect causes a red shift of the axial C−H stretch frequency, as was observed experimentally and reproduced in our ab initio calculations.[76] A similar red shift is therefore expected to occur for adsorbed cyclohexadienyl. A long *equatorial* C−H bond is also found for this cyclohexadienyl species. This is caused by interaction of the H-atom with a surface Pt-atom; the distance to the Pt-atom is quite short and the position of the hydrogen atom is directly above the Pt-atom (Figure 3).

The first step has an activation energy of 100 kJ/mol. The drop of 29 kJ/mol in the potential energy surface is due to the formation of the tilted intermediate state. The barrier from the tilted intermediate to the cyclohexadienyl product is much lower at 11−41 kJ/mol. Whether the first or the second barrier is the highest point along the reaction path depends on the inclusion

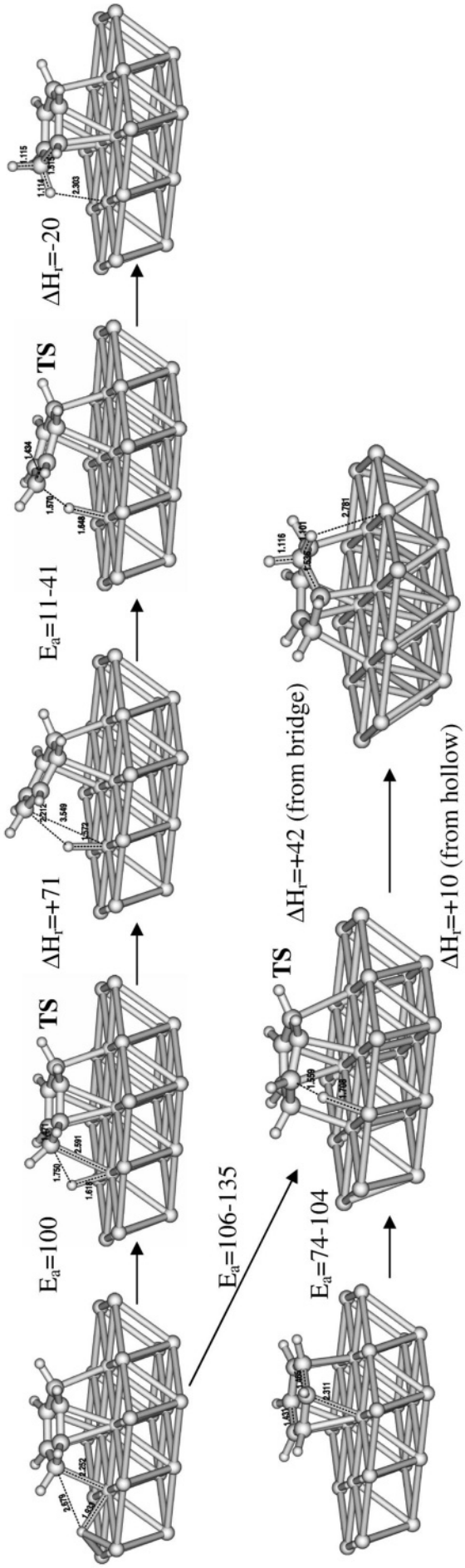

Figure 3. Different reaction paths for the addition of the first hydrogen atom. The hydrogenation activation energies and enthalpies of reaction are listed (kJ/mol). Bond distances in ångstroms.

of the ZPE, but the difference is small in either case. The overall reaction is endothermic by +51 kJ/mol. The fairly shallow depth of the minimum for the intermediate state suggests that the intermediate has a very short lifetime.

In the section 3.4 on the addition of the second H-atom, reactions having a similar "three-centered" mechanism will be discussed. In these cases a one step mechanism is found. Also in the case of ethene hydrogenation a one step "three-centered" mechanism is found.[87] The occurrence of two steps here is caused by two factors. A first factor is the strength of the C_1-Pt bond that has to be broken. The strong interaction of C_1 with the Pt-atom underneath has been discussed in our paper on benzene adsorption.[75] Second, in the intermediate the benzene molecule can restore part of its aromatic stability. This is indicated from the shortening of the C_1-C bonds from 148 pm for the adsorbed benzene to a value comparable to the value in gas-phase benzene (140 pm). In the second step, this regained aromatic stability has to be overcome to add the hydrogen atom, giving rise to the second barrier. This effect is related to aromaticity and is therefore not observed in ethene hydrogenation. It is, however, obvious that those two effects are very subtle.

Addition of hydrogen to C_2 follows a very different pathway (Figure 3). In the transition state the C_2-Pt bond is already broken and a C_2-H bond is being formed. In this case no reaction intermediate is found. The C_2-H and H−Pt distances are similar to the values for the second transition state of the first reaction path. This indicates that the C_2-Pt bond is more easily broken than the C_1-Pt bond. The higher strength of the C_1-Pt bond was also discussed in our paper on benzene adsorption.[75] A similar transition state geometry is found for the hydrogenation of π-bound ethene on Pd(111)[87] at higher surface coverage. At lower coverage the approaching H-atom pushes the ethene molecule to the more stable di-σ-bound mode. The benzene molecule is, however, held at the bridge site by five additional C−Pt bonds and cannot be "pushed away". This mechanism is called a "slip" mechanism, whereby the C−C bond slides upward to form a "five-center like" transition state.[87] There are, however, distinct differences between the ethene and benzene transition state geometry. For ethene hydrogenation the attacking hydrogen atom is at the bridge site to yield optimal orbital overlap with the ethene π-orbital in the transition state. For benzene hydrogenation the attacking hydrogen cannot bind to the similar bridge site, because the benzene molecule is still bound to the second Pt atoms of this bridge site. Moreover, the presence of the benzene ring limits the flexibility, making the reaction more difficult.

The cyclohexadienyl product is distinct from the one formed via the first path. The axial C−H bond is again lengthened for similar reasons as for the cyclohexadienyl product from the "three-centered" mechanism. The equatorial C−H bond, however, has a normal length because the distance from the equatorial H-atom to a Pt-atom is large, indicating there is no interaction with the surface.

An activation barrier of 106−135 kJ/mol was calculated, which is slightly higher than for the "three-centered" mechanism. In ethene hydrogenation over Pd(111) the activation barrier for the "slip" mechanism is about 50 kJ/mol lower than for the "three-centered" mechanism. However, in ethene hydrogenation, the reactants for the two mechanisms are different: the "slip" mechanism starts from the π-bound species, whereas the "three-center" mechanism starts from the more stable di-σ-bound ethene. In benzene hydrogenation both mechanisms start from the bridge-bound species.

Hollow-bound benzene has a low barrier for surface diffusion and is therefore quite mobile. During the initial scan of the potential energy surface to locate a transition state, the benzene molecule moves and a transition state is found that is identical to that for the "slip" mechanism for the hydrogenation of bridge-bound benzene. In this set of calculations, the energy increased monotonically until the transition state was reached, indicating that a genuine transition state was located. The hollow-bound benzene reactant state is less stable than the bridge-bound benzene, which leads to a lower activation energy of 74−104 kJ/mol. The hydrogenation is found to be endothermic by +10 kJ/mol.

Therefore, the weakly adsorbed hollow site benzene is more likely to be the reactive species, whereas the bridge site species may be too strongly adsorbed and can likely be regarded as a spectator species. As discussed in section 3.1, the relative surface concentration varies with coverage. In the present work, the adsorption enthalpies are calculated for very low coverage and low temperature. At temperatures and pressures that are more consistent with the industrial reaction conditions other factors begin to strongly influence the relative concentrations. Higher pressures lead to higher surface coverage, which favors benzene adsorption at the hollow sites (section 3.1).

3.4. Addition of the Second Hydrogen Atom. As discussed, two types of cyclohexadienyl species can be formed. Only the hydrogenation of the cyclohexadienyl species formed from hollow-bound benzene was studied. The other cyclohexadienyl intermediate is not considered for two reasons. Kinetically, the activation barrier to form the latter is about 26 kJ/mol higher and, thermodynamically, the overall reaction enthalpy for it to form is 41 kJ/mol more endothermic (+51 kJ/mol vs +10 kJ/mol). In other words, the hydrogenation of hollow-bound benzene is the dominant reaction path for the addition of the first hydrogen atom.

The adsorbed cyclohexadienyl intermediate has five inequivalent carbon atoms. The transition states and products for the five reaction paths are shown in Figure 4, together with the activation energies and the reaction enthalpies. To distinguish the different reaction paths, names are chosen to indicate the position of the hydrogen addition. So we use 1,2-dihydrobenzene (12DHB) and 1,6-dihydrobenzene (16DHB), which correspond to the same product, i.e., adsorbed 1,3-cyclohexadiene.

First, we discuss the different reaction paths in detail. 14DHB is the most stable form of adsorbed 1,4-cyclohexadiene. The adsorption and the frequency spectrum of 1,4-cyclohexadiene have been described in a previous communication.[76] Other, less favored adsorption geometries have been discussed there as well, but they are not formed via the hydrogenation mechanism discussed here. The calculated adsorption energy for 1,4-cyclohexadiene of −146 kJ/mol is in good agreement with the value of −142 kJ/mol suggested by Koel et al.[68] The axial C−H bonds are lengthened in comparison with the gas-phase values of 110.8 pm due to through bond interaction in combination with strong electron donation from the axial σCH bond to the metal.[76] Hydrogenation to form 1,4-cyclohexadiene has a high activation energy of 115−138 kJ/mol.

Two of the identified reaction paths in Figure 4 lead to the formation of adsorbed 1,3-dihydrobenzene. Two different orientations are found: 13DHB and 15DHB. Closer inspection shows that 13DHB and 15DHB are identical, except for their orientation with respect to the Pt-cluster. In 15DHB, the CH_2 groups are closer to the cluster's edges, giving a slightly higher binding strength, which can be attributed to a cluster size effect. The adsorbed species have two long axial C−H bonds, caused

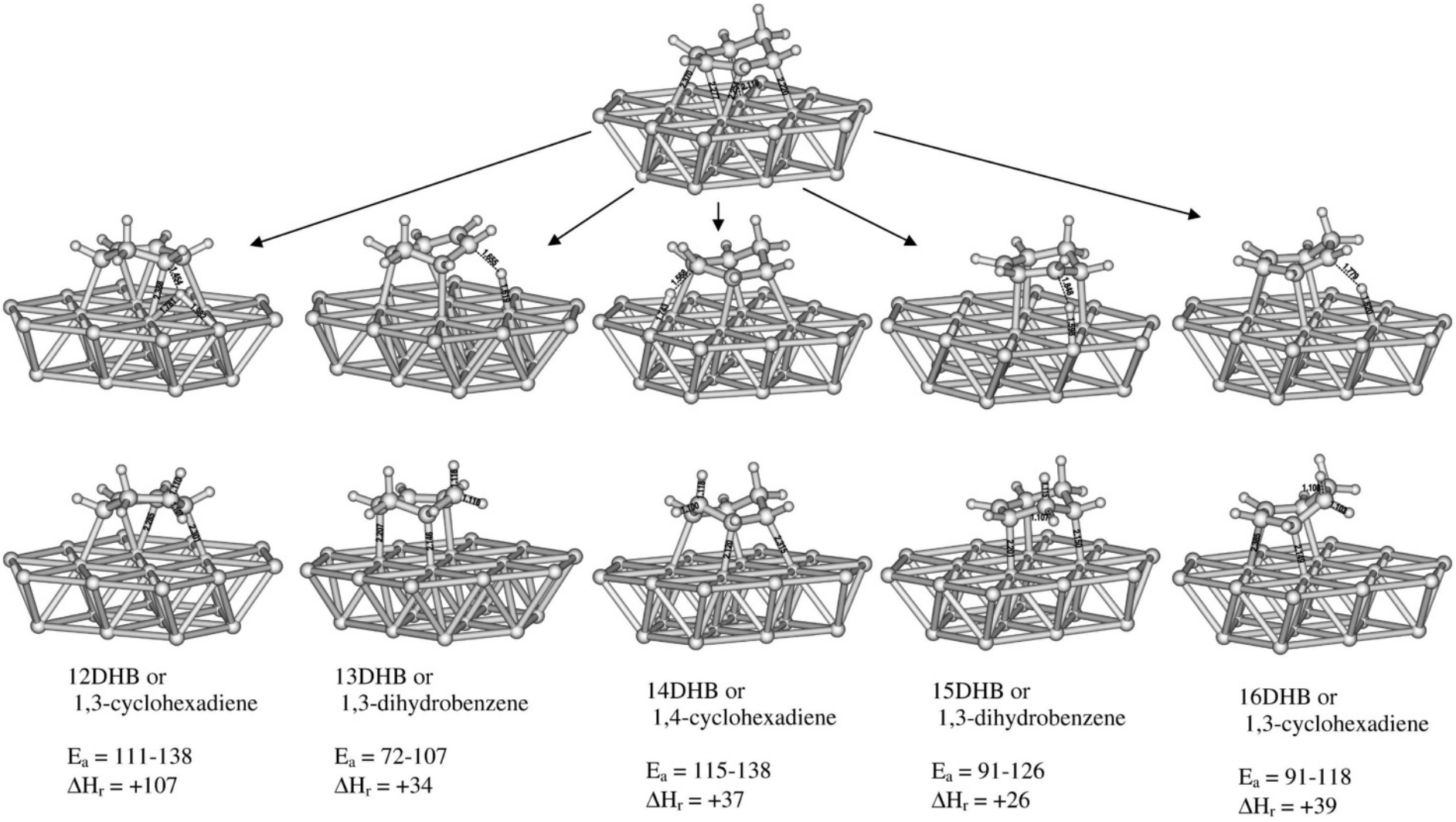

Figure 4. Five reaction paths for the addition of the second hydrogen atom. The names of the intermediates, the hydrogenation activation energies and enthalpies of reaction are listed (kJ/mol). Bond distances in ångstroms.

by a similar effect as for adsorbed 1,4-cyclohexadiene. These reactions are the least endothermic, by +26−34 kJ/mol, among the five hydrogenation paths identified. They also have the lowest activation barriers. Thus, the dominant reaction path goes via the formation of the 13DHB surface intermediate. The cyclohexadienyl C−Pt bond that is hydrogenated in this path is substantially longer, i.e., weaker, than the four other C−Pt bonds (Figure 4). This in part explains the low barrier for this path.

12DHB and 16DHB are two forms of adsorbed 1,3-cyclohexadiene. An adsorption energy of −143 kJ/mol was calculated for the most stable form. No direct experimental value is available, because 1,3-cyclohexadiene dehydrogenates before it can desorb.[51,52,57−62] On the basis of quasi-valence-bond theory, Koel et al.[68] estimated an adsorption enthalpy of −142 kJ/mol, which agrees with our calculated value. The axial C−H bond length is similar to the gas-phase value, which is in agreement with the fact that no red shift of the C−H stretch frequency is observed experimentally.[61] The through-bond interaction that occurs for 1,4-cyclohexadiene, cyclohexadienyl, and 1,3-dihydrobenzene does not occur for 1,3-cyclohexadiene. An intermediate activation barrier of 91−117 kJ/mol is associated with the hydrogenation to form the more stable 16DHB. The reaction is +38 kJ/mol endothermic. The formation of 12DHB is difficult. A high activation energy of 116−142 kJ/mol and a high endothermicity of +106 kJ/mol are calculated. The strong C−Pt bond that has to be broken can explain this. In cyclohexadienyl, the corresponding C−Pt bond is significantly shorter than the others.

As for the addition of the first hydrogen atom, two mechanisms can be distinguished. Hydrogenation to form 13DHB and 16DHB goes via the "three-centered" mechanism; i.e., the attacking H-atom moves over a Pt-atom. Here, this is a one step mechanism. No transition state corresponding to the breaking of the C−Pt bond -the first step in bridge-bound benzene C_1 hydrogenation is found. Less C−Pt bonds are affected during the hydrogenation step, causing a smaller increase of the energy along the reaction path. Therefore, no corresponding barrier is found. Hydrogenation to 14DHB and 15DHB occurs via a "slip" mechanism. Hydrogenation to 12DHB also goes via a "slip"-like mechanism, but the transition state looks quite different. A short, i.e., strong, C−Pt bond has to be broken, leading to a substantial barrier and a late transition state.

There are two factors that determine the activation energy. First, the position at which the hydrogenation occurs is important. The activation energy to form 1,3-dihydrobenzene (either 13DHB or 15DHB) is about 20 kJ/mol lower than that to form 1,3-cyclohexadiene or 1,4-cyclohexadiene, for a similar hydrogenation mechanism. Adsorbed 1,3-dihydrobenzene is also 10−12 kJ/mol more stable than adsorbed 1,3- and 1,4-cyclohexadiene. Second, the specific reaction coordinate that dictates the mechanism is important. The activation energy for the "slip" mechanism is about 20 kJ/mol higher than that for the "three-centered" mechanism. This can be seen by comparing the barrier to form 16DHB and 12DHB. In the former, 1,3-cyclohexadiene is formed via the three-center mechanism, for the latter it is formed via the slip mechanism. Comparing the barriers to form 13DHB (three-centered mechanism) and 15DHB ("slip" mechanism) confirms this observation. The hydrogenation to form 14DHB (i.e., 1,4-cyclohexadiene) also follows a "slip" mechanism, and thus the high barrier is expected. Also, for the hydrogenation of bridge-bound benzene, the two mechanisms can also be compared. Again, the activation barrier for the "slip" mechanism is 25 kJ/mol higher than that for the "three-centered" mechanism (the second transition state).

3.5. Dehydrogenation. Some kinetic models for benzene hydrogenation include the presence of a dehydrogenated species.[19−21,36] The intermediates are typically assumed to be the most abundant surface intermediates. During benzene TPD studies no desorption is observed at low coverage; all the benzene dehydrogenates.[59,62,63] From these studies an activation energy for benzene dehydrogenation of 117−138 kJ/mol is found. Cabibil et al.[67] studied the thermal chemistry of iodobenzene on Pt. They found that upon heating the formed phenyl species readily disproportionated into benzene and *o*-benzyne. No biphenyl formation was observed. In some experiments a tilted phenyl species was observed with HREELS.[67]

The formation of phenyl and *o*-, *m*-, and *p*-benzyne species from bridge- and hollow-bound benzene was studied in the present work. The products are shown in Figure 5 along with the corresponding reaction enthalpies. All dehydrogenation reactions from benzene to phenyl and adsorbed hydrogen were found to be highly endothermic. For the bridge-bound benzene, we examined dehydrogenation at the C_1 and at the C_2 carbon centers (Figure 2). Dehydrogenation at C_2 is endothermic by +168 kJ/mol. In the product species, the C_2 carbon atom is unsaturated. It cannot compensate for the loss of a C−H bond by forming an extra C−Pt bond. The high endothermicity in comparison with the desorption energy prohibits this reaction. Benzene will rather desorb than dehydrogenate to this phenyl species. Dehydrogenation at C_1 leads to two forms of phenyl, a vertical form and a tilted form. A flat orientation was tested, but it relaxed to the tilted geometry during the calculation. The tilted form is about 10 kJ/mol preferred over the vertical form. Because the rotational entropy is higher for the vertical orientation, the relative concentration will likely change with temperature. For the tilted form an angle of 38° with respect to the Pt surface is found. Experimentally, a tilting angle of 73° was predicted from the relative intensities of the $C-H_{in\text{-}plane}$ and $C-H_{out\text{-}of\text{-}plane}$ bending modes in the HREELS spectrum.[67] It is, however, likely that under the experimental conditions both the tilted and vertical phenyl species will be present, leading to the observation of an intermediate value. The endothermicity of this reaction amounts to +76 kJ/mol. This is lower than the desorption energy of bridge-bound benzene, but still strongly endothermic. Dehydrogenation of hollow-bound benzene is endothermic by +50 kJ/mol. This is also lower than the desorption energy of +71 kJ/mol. Considering that the hydrogen adsorption enthalpy decreases strongly with increasing coverage,[104] the endothermicity of these reactions will increase even more at higher coverage.

All benzene dehydrogenation reactions were found to be highly endothermic. From thermodynamic considerations, only negligible surface concentration of phenyl will be present under hydrogenation conditions. However, under UHV conditions, benzene dehydrogenation is observed experimentally. Although the dehydrogenation reactions are found to be endothermic, the endothermicity is lower than the desorption enthalpy. No activation energies for dehydrogenation were calculated, but if the activation energy for dehydrogenation is not too much higher than the corresponding reaction endothermicity, but still lower than the desorption energy, and if the preexponential factors for dehydrogenation and desorption are of the same order of magnitude, dehydrogenation should occur. Under UHV conditions and at the temperature at which dehydrogenation occurs in the TPD studies, the hydrogen atoms that result desorb as

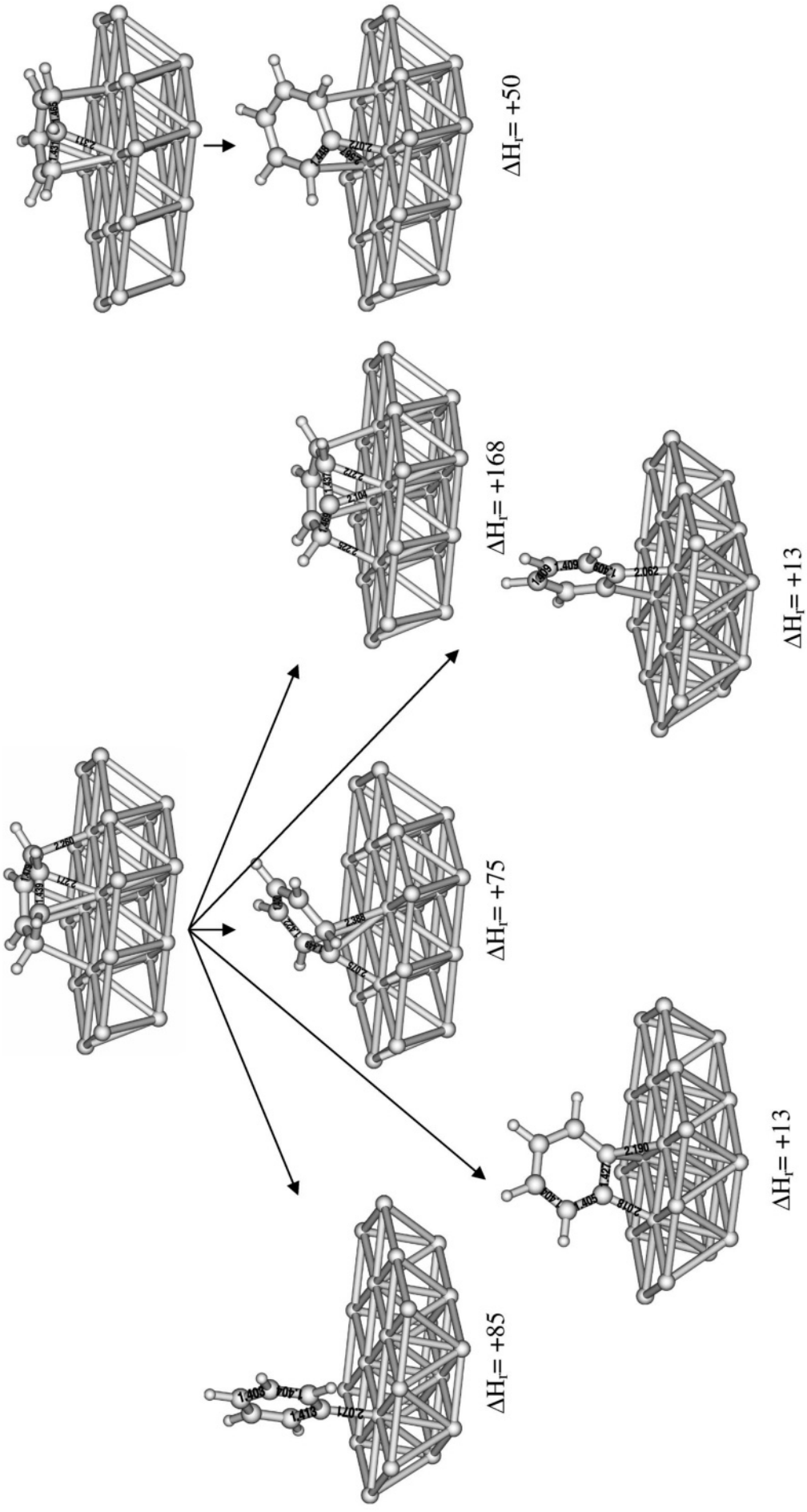

Figure 5. Different reaction paths for the dehydrogenation of benzene. The enthalpies of reaction with respect to benzene are listed (kJ/mol). Bond distances in ångstroms.

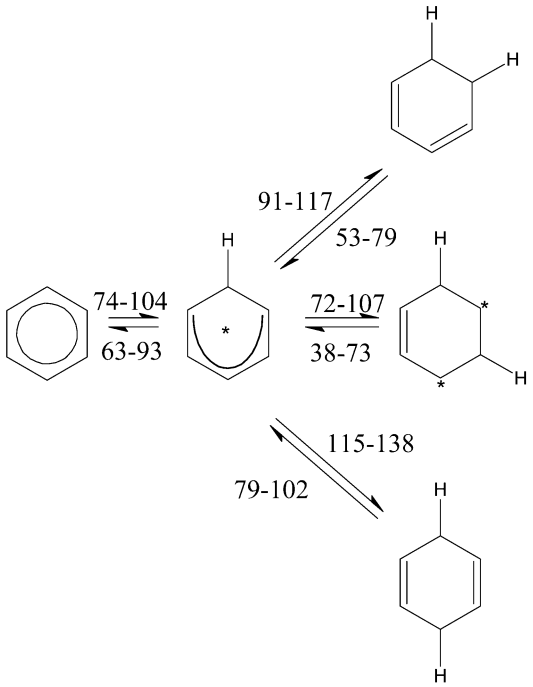

Figure 6. Summary of calculated kinetic parameters (kJ/mol).

they are formed and the equilibrium is shifted to the side of the dehydrogenated product.

To verify that there are no further dehydrogenated species that are more stable on the surface, we examined the dehydrogenation of phenyl to benzyne species. Calculations with small Pt-clusters showed that adsorbed *p*-benzyne is +160 kJ/mol less stable than *o*-benzyne and *m*-benzyne is +200 kJ/mol less preferred. Therefore, only the adsorption of *o*-benzyne was studied on the larger cluster. The formation of *o*-benzyne from phenyl was found to be exothermic. Two possible orientations were found starting from different phenyl species (Figure 5). In both geometries, the benzyne ring was found to be perpendicular to the surface. In one case, the benzyne triple bond was adsorbed at the hollow site leading to a calculated adsorption energy of −374 kJ/mol. Adsorption at the bridge site has the same calculated adsorption energy. Similar results were obtained for acetylene adsorption on Cu(111) and Pd(111).[110] With respect to bridge-bound benzene, the reaction to adsorbed *o*-benzyne and two hydrogen atoms is still endothermic by +13 kJ/mol. Again, the endothermicity is dependent on the dihydrogen enthalpy of adsorption. At high coverage $\Delta H^0_{ads}(H_2)$ decreases from −95 to −45 kJ/mol and the endothermicity of the dehydrogenation increases to +63 kJ/mol.

The calculated enthalpies of reaction are also consistent with the observed disproportionation of phenyl to *o*-benzyne and benzene.[67]

4. Consequences for the Reaction Path of Benzene Hydrogenation

In this section the results from the ab initio calculations will be used to provide insight in the first steps of the hydrogenation of benzene over platinum. The calculated activation energies are summarized in Figure 6. As discussed in the Computational Methods section, two activation energies are listed. The low values correspond to the hypothesis that the hydrogenation barrier is equal to the electronic energy barrier or, stated differently, that the ZPE of the transition state is equal to the ZPE of the reactants. The high values correspond with the hypothesis that the dehydrogenation barrier is equal to the electronic energy barrier. We believe the low value is closer to the reality than the high value.

There are two forms of adsorbed benzene present on the surface. Their relative concentration depends on the total surface coverage and the temperature and thus on the process conditions. Bridge-bound benzene is strongly adsorbed on Pt(111). It has a relatively high barrier for diffusion and in addition a high activation energy for hydrogenation. It is therefore rather inert. Hollow-bound benzene, however, is less strongly bound to the surface. It is therefore more mobile on the surface than bridge-bound benzene and has a barrier for hydrogenation that is about 20 kJ/mol lower than that for the bridge-bound intermediate. Therefore, the hollow-bound benzene intermediate is more likely the reactive surface species. This is similar to the observation for ethene hydrogenation, where the weakly π-bound species is believed to be the reactive species, whereas the strongly di-σ-bound species is believed not to participate in the hydrogenation reaction.[57]

The addition of the first hydrogen atom has a calculated barrier of 74−104 kJ/mol and is endothermic by +11 kJ/mol. The addition of the second hydrogen atom can lead to three different products. The kinetically and thermodynamically favored path has an activation energy of 72−107 kJ/mol and proceeds via the formation of 1,3-dihydrobenzene. This species would be a highly unstable diradical in the gas phase. On the surface, however, it is the most stable dihydrogenated product. The barrier to adsorbed 1,3-cyclohexadiene is 19 kJ/mol higher, and the barrier to adsorbed 1,4-cyclohexadiene is 43 kJ/mol higher. Therefore the reaction path via 1,3-dihydrobenzene is more likely the dominant reaction path.

The activation energy for the addition of the second hydrogen atom is essentially equal to the activation energy for the addition of the first hydrogen. In some kinetic models, it has been assumed that the addition of the first hydrogen atom to benzene is the rate determining step.[19−21,25,36] The reasoning has been that in the first step the aromaticity of the benzene molecule has to be broken and that therefore this step is the most difficult one. Our calculations show that this is not the case. The addition of the first and second hydrogen atom have similar activation barriers. By simply examining the adsorption enthalpies of cyclohexene, i.e., −72 kJ/mol,[68] and cyclohexadiene, i.e., −146 kJ/mol,[68] one would expect benzene to have an adsorption enthalpy of −218 kJ/mol. The adsorption enthalpy of benzene at the hollow site, however, is −71 kJ/mol, a difference of 147 kJ/mol. The reason for this difference can be explained in part by the loss of resonance energy by benzene upon adsorption. This resonance energy amounts to 150 kJ/mol. An indication of the loss of aromaticity upon adsorption is that different C−C bond lengths are found in the adsorbed benzene ring (Figure 2). In our orbital analysis of benzene adsorption[75] we found that the π-orbitals undergo substantial donation and back-donation with the platinum d-orbitals, which in turn can destroy the aromaticity of benzene. This could explain the similarity in activation energy for the first and second hydrogen atom.

From the calculated energy diagram, some insight in the reaction rate of the addition of the first and the second hydrogen atom can be obtained. If we assume that the addition of the first hydrogen atom is quasi-equilibrated, then, because of the endothermicity of this reaction, the surface concentration of the cyclohexadienyl product is lower than that of benzene. The addition of the second hydrogen atom has a similar activation energy as the addition of the first. If also the preexponential factors are similar, then the rate coefficients are similar. Because

the rate of reaction is the product of the rate coefficient and the reactant concentration, the addition the second hydrogen atom has a lower rate than the addition of the first, and would become potentially rate-determining.

5. Comparison with Observations on Platinum Single Crystals

Most surface science studies over platinum single crystals reported in the literature have focused on dehydrogenation reaction paths, as they are somewhat easier to perform than hydrogenation studies. In the next few paragraphs, we compare the experimental findings for 1,3- and 1,4-cyclohexadiene dehydrogenation[52,53,58−61] with the calculated potential energy diagram in Figure 6. For 1,3-cyclohexadiene dehydrogenation a barrier between 50 and 69 kJ/mol[52,58−61] was found experimentally. This agrees reasonably well with our ab initio values. The agreement is best with the lower of the calculated values, which are preferred on physical grounds as well. Some studies have compared 1,3-cyclohexadiene dehydrogenation with 1,4-cyclohexadiene dehydrogenation.[52,59,61] The latter is found to dehydrogenate more slowly than 1,3-cyclohexadiene, with an activation barrier between 65 and 74 kJ/mol, again in agreement with our lower value. The reported experimental values are obtained from temperature programmed (TP) reaction studies.

During the TP dehydrogenation of 1,3-cyclohexadiene, an intermediate has been observed in a narrow temperature window by vibrational spectroscopy.[52,61] No intermediate was observed in 1,4-cyclohexadiene dehydrogenation. This intermediate has a low C−H stretch frequency; similar to the frequency observed for adsorbed 1,4-cyclohexadiene. In publications from Somorjai and co-workers[57,58,61] it is speculated that 1,3-cyclohexadiene is converted 1,4-cyclohexadiene before it dehydrogenates. Manner et al.[52] suggest, however, that the observed intermediate is a cyclohexadienyl species. Our results support the latter assignment. The barrier for 1,3-cyclohexadiene to lose its first H-atom is 10−14 kJ/mol lower than the barrier to lose its second H-atom. Thus there should be a 40−50 K temperature window in which this intermediate is observable, which is indeed what is seen experimentally. As explained in the previous section, the axial C−H bond in cyclohexadienyl is stretched, and a red shift of the C−H stretch frequency is expected.

From our calculated barriers, a cyclohexadienyl intermediate is not expected to occur during the dehyrogenation of adsorbed 1,4-cyclohexadiene. Here, the barrier to lose the first hydrogen is higher than the barrier to lose the second. When the temperature is high enough to surmount the barrier for the first dehydrogenation step, it is high enough to surmount the second barrier as well, especially because the reaction is exothermic.

6. Conclusions

A detailed density functional analysis was performed to gain a more atomic level understanding of the mechanism of benzene hydrogenation on platinum catalysts. The cluster calculations presented in this paper correspond to low coverages on the (111) surface of a platinum catalyst. It was found that it is important to include the zero point vibrational energy and the internal energies due to translation, vibrational motion and rotational motion to obtain more accurate enthalpies for (de)hydrogenation reactions-in this paper we propose an efficient methodology to calculate these thermal corrections. The reaction path analysis was carried out on the basis of the enthalpy profile and entropy contributions were not considered.

There are two sites for benzene adsorption. Benzene adsorbed at the hollow site is the reactive species, whereas benzene adsorbed at the bridge site was found to be too stable to react. For the addition of the first hydrogen atom an activation energy of 74−104 kJ/mol was calculated. The dominant reaction path for the addition of the second hydrogen atom proceeds via 1,3-dihydrobenzene. This path has a substantially lower activation barrier than the mechanisms via 1,3-cyclohexadiene and 1,4-cyclohexadiene, which are therefore not likely intermediates in the benzene hydrogenation. The barrier for the addition of the second hydrogen atom is similar to barrier for the addition of the first hydrogen atom, i.e., 72−107 kJ/mol.

Two types of mechanisms were observed, i.e., a "three-centered" mechanism in which the attacking hydrogen atom moves over a platinum atom and a "slip" mechanism that passes through a five-centered transition state. The barrier for the "three-centered" mechanism is found to be 20 kJ/mol lower than the barrier for the "slip" mechanism.

The calculated barrier for 1,3-cyclohexadiene dehydrogenation is 53−79 kJ/mol, for 1,4-cyclohexadiene it is 79−102 kJ/mol. These results are in qualitative and quantitative agreement with experimental data. The calculations confirm the existence of an intermediate species during 1,3-cyclohexadiene TPR in a 40−50 K temperature window. From the calculations it follows that this intermediate is adsorbed cyclohexadienyl.

The dehydrogenation of benzene to phenyl is +76 kJ/mol endothermic. This step is therefore thermodynamically and kinetically not favorable. Further dehydrogenation to *o*-benzyne is still +14 kJ/mol endothermic with respect to benzene. Dehydrogenation is therefore an irreversible side reaction during benzene hydrogenation and should not be included in a kinetic model for benzene hydrogenation.

In conclusion, the results presented here were in reasonable agreement with experimental information and therefore theory begins to provide yet another tool by which to investigate surface chemistry for industrial catalytic systems.

Acknowledgment. We thank Venkataram Pallassana for his help in setting up the calculations reported herein and Joris Thybaut for useful discussions. M.S. is grateful to the Fund for Scientific Research-Flanders, Belgium (F.W.O.-Vlaanderen) for a Research Assistantship. This research was carried out in the framework of "InterUniversity Attraction Poles", funded by the Belgian government and the DWTC office.

References and Notes

(1) Somorjai, G. A. *Chemistry in Two Dimensions: Surfaces*; Cornell University Press: Ithaca, NY, 1981.

(2) Satterfield, C. N. *Heterogeneous Catalysis in Industrial Practice*, 2nd ed.; McGraw-Hill: New York, 1991.

(3) Davis, S. M.; Somorjai, G. A. In *The Chemical Physics of Solid Surfaces and Heterogeneous Catalysis*; King, D. A., Woodruff, D. P., Eds.; Elsevier: Amsterdam, 1984; Vol. 4.

(4) http://www.eia.doe.gov/pub/international/ieapdf/t03_06.pdf

(5) Schuller, M.; Hodges, P. In *Proceedings of the DGMK-conference "The Future Role of Aromatics in Refining and Petrochemistry"*; Emig, G., Rupp, M., Weitkamp, J., Eds.; Erlangen, 1999; p 21.

(6) Cooper, B. H.; Donnis, B. B. L. *Appl. Catal. A: Gen.* **1996**, *137*, 203.

(7) http://www.apme.org/media/public_documents/20010821_115044/46.pdf

(8) Smeds, S.; Salmi, T.; Murzin, D. Y. *React. Kinet. Catal.* **1998**, *L63*, 47.

(9) Keane, M. A.; Patterson, P. M. *Ind. Eng. Chem. Res.* **1999**, *38*, 1295.

(10) Keane, M. A.; Patterson, P. M. *J. Chem. Soc., Faraday Trans.* **1996**, *92*, 1413.

(11) Au, S. S.; Dranoff, J. S.; Butt, J. B. *Chem. Eng. Sci.* **1995**, *50*, 3801.

(12) Reyes, P.; Concha, I.; Konig, M. E.; Delgado, E. *Bol. Soc. Chil. Quim.* **1991**, *36*, 147.

(13) Ostrovskii, N. M.; Parmaliana, A.; Frusteri, F.; Maslova, L. P.; Giordano, N. *Kinet. Catal.* **1991**, *32*, 67.
(14) Coughlan, B.; Keane, M. A. *Zeolites* **1991**, *11*, 483.
(15) Coughlan, B.; Keane, M. A. *Zeolites* **1991**, *11*, 12.
(16) Chou, P.; Vannice, M. A. *J. Catal.* **1987**, *107*, 140.
(17) Yoon, K. J.; Vannice, M. A. *J. Catal.* **1983**, *82*, 457.
(18) Singh, U. K.; Vannice, M. A. *AIChE J.* **1999**, *45*, 1059.
(19) Lin, S. D.; Vannice, M. A. *J. Catal.* **1993**, *143*, 539.
(20) Lin, S. D.; Vannice, M. A. *J. Catal.* **1993**, *143*, 563.
(21) Tétényi, P. *J. Catal.* **1994**, *147*, 601.
(22) Lafyatis, D. S.; Creten, G.; Dewaele, O.; Froment, G. F. *Can. J. Chem. Eng.* **1997**, *75*, 1100.
(23) Mirodatos, C.; Dalmon, J. A.; Martin, G. A. *J. Catal.* **1987**, *105*, 405.
(24) Van Meerten, R. Z. C.; Coenen, J. W. E. *J. Catal.* **1977**, *46*, 13.
(25) Schoenmaker-Stolk, M. C.; Verwijs, J. W.; Don, J. A.; Scholten, J. J. F. *Appl. Catal.* **1987**, *29*, 73.
(26) Parmaliani, A.; El Sawi, M.; Mento, G.; Fedele, U.; Giordano, N. *Appl. Catal.* **1983**, *7*, 221.
(27) Primet, M.; Garbowski, E.; Mathieu, M. V.; Imelik, B. *J. Chem. Soc., Faraday Trans. 1* **1980**, *76*, 1953.
(28) Sica, A. M.; Valles, E. M.; Gigola, C. E. *J. Catal.* **1978**, *51*, 115.
(29) Germain, J. E.; Bourgeois, Y. *Bull. Soc. Chim. Fr.* **1960**, 2127.
(30) Derbentsev, Y. I.; Paal, Z.; Tétényi, P. *Z. Phys. Chem. N. F.* **1972**, *80*, 51.
(31) Thybaut, J. W.; Saeys, M.; Marin, G. B. *Chem. Eng. J.*, in press.
(32) Rousset, J. L.; Stievano, L.; Aires, F. J. C. S.; Geantet, C.; Renouprez, A. J.; Pellarin, M. *J. Catal.* **2001**, *197*, 335.
(33) Chupin, J.; Gnep, N. S.; Lacombe, S.; Guisnet, M. *Appl. Catal. A: Gen.* **2001**, *206*, 43.
(34) Lindfors, L. P.; Salmi, T.; Smeds, S. *Chem. Eng. Sci.* **1993**, *48*, 3813.
(35) Lindfors, L. P.; Salmi, T. *Ind. Eng. Chem. Res.* **1993**, *32*, 34.
(36) Lin, S. D.; Vannice, M. A. *J. Catal.* **1993**, *143*, 554.
(37) Smeds, S.; Salmi, T.; Murzin, D. Y. *Appl. Catal. A: Gen.* **2000**, *201*, 55.
(38) Smeds, S.; Murzin, D.; Salmi, T. *Appl. Catal. A: Gen.* **1996**, *141*, 207.
(39) Smeds, S.; Murzin, D.; Salmi, T. *Appl. Catal. A: Gen.* **1997**, *150*, 115.
(40) Keane, M. A. *J. Catal.* **1997**, *166*, 347.
(41) Huang, T. C.; Kang, B. C. *Ind. Eng. Chem. Res.* **1995**, *34*, 1140.
(42) Rahaman, M. V.; Vannice, M. A. *J. Catal.* **1991**, *127*, 267.
(43) Bussell, M. E.; Henn, F. C.; Campbell, C. T. *J. Phys. Chem.* **1992**, *96*, 5978.
(44) Parker, D. H.; Pettiette-Hall, C. L.; Li, Y.; McIver, R. T.; Hemminger, J. C. *J. Phys. Chem.* **1992**, *96*, 1888.
(45) Land, D. P.; Pettiette-Hall, C. L.; McIver, R. T.; Hemminger, J. C. *J. Am. Chem. Soc.* **1989**, *111*, 5970.
(46) Land, D. P.; Erley, W.; Ibach, H. *Surf. Sci.* **1993**, *289*, 237.
(47) Parker, D. H.; Pettiette-Hall, C. L.; Li, Y. Z.; McIver, R. T.; Hemminger, J. C. *J. Phys. Chem.* **1992**, *96*, 1888.
(48) Pettiette-Hall, C. L.; Land, D. P.; McIver, R. T.; Hemminger, J. C. *J. Am. Chem. Soc.* **1991**, *113*, 2755.
(49) Rodriguez, J. A.; Campbell, C. T. *J. Phys. Chem.* **1989**, *93*, 826.
(50) Xu, C.; Tsai, Y.-L.; Koel, B. E. *J. Phys. Chem.* **1994**, *98*, 585.
(51) Gland, J. L.; Baron, K.; Somorjai, G. A. *J. Catal.* **1975**, *36*, 305.
(52) Manner, W. L.; Girolami, G. S.; Nuzzo, R. G. *J. Phys. Chem. B* **1998**, *102*, 10295.
(53) Tsai, M. C.; Friend, C. M.; Meutterties, E. L. *J. Am. Chem. Soc.* **1982**, *104*, 2539.
(54) Henn, F. C.; Diaz, A. L.; Bussell, M. E.; Hugenschmidt, M. B.; Domagala, M. E.; Campbell, C. T. *J. Phys. Chem.* **1992**, *96*, 5965.
(55) McCrea, K. R.; Somorjai, G. A. *J. Mol. Catal. A: Chem.* **2000**, *163*, 43.
(56) Rodriguez, J. A.; Campbell, C. T. *J. Catal.* **1989**, *115*, 500.
(57) Somorjai, G. A.; Rupprechter, G. *J. Phys. Chem. B* **1999**, *103*, 1623.
(58) Su, X.; Kung, K. Y.; Lahtinen, J.; Shen, Y. R.; Somorjai, G. A. *J. Mol. Catal. A: Chem.* **1999**, *141*, 9.
(59) Hugenschmidt, M. B.; Diaz, A. L.; Campbell, C. T. *J. Phys. Chem.* **1992**, *96*, 5974.
(60) Peck, J. W.; Koel, B. E. *J. Am. Chem. Soc.* **1996**, *118*, 2708.
(61) Su, X.; Shen, Y. R.; Somorjai, G. A. *Chem. Phys. Lett.* **1997**, *280*, 302.
(62) Campbell, C. T.; Campbell, J. M.; Dalton, P. J.; Henn, F. C.; Rodriguez, J. A.; Seimanides, S. G. *J. Phys. Chem.* **1989**, *93*, 806.
(63) Campbell, J. M.; Seimanides, S. G.; Campbell, C. T. *J. Phys. Chem.* **1989**, *93*, 815.
(64) Haq, S.; King, D. A. *J. Phys. Chem.* **1996**, *100*, 16957.
(65) Lehwald, S.; Ibach, H.; Demuth, J. E. *Surf. Sci.* **1978**, *78*, 577.
(66) Tsai, M. C.; Muetterties, E. L. *J. Am. Chem. Soc.* **1982**, *104*, 2534.
(67) Cabibil, H.; Ihm, H.; White, J. M. *Surf. Sci.* **2000**, *447*, 91.
(68) Koel, B. E.; Blank, D. A.; Carter, E. A. *J. Mol. Catal. A: Chem.* **1998**, *131*, 39.
(69) Kang, D. B.; Anderson, A. B. *J. Am. Chem. Soc.* **1985**, *107*, 7858.
(70) Sautet, P.; Bocquet, M.-L. *Phys. Rev. B* **1996**, *53*, 4910.
(71) Kryachko, E. S.; Arbuznikov, A. V.; Hendrickx, M. F. A. *J. Phys. Chem. B* **2001**, *105*, 3557.
(72) Roszak, S.; Balasubramanian, K. *Chem. Phys. Lett.* **1995**, *234*, 101.
(73) Majumdar, D.; Roszak, S.; Balasubramanian, K. *J. Chem. Phys.* **2001**, *114*, 10300.
(74) Ohno, M.; von Niessen, W. *Surf. Sci.* **1997**, *388*, 276.
(75) Saeys, M.; Reyniers, M.-F.; Marin, G. B.; Neurock, M. *J. Phys. Chem. B* **2002**, *106*, 7489.
(76) Saeys, M.; Reyniers, M.-F.; Marin, G. B.; Neurock, M. *Surf. Sci.* **2002**, *513*, 315.
(77) Yamagishi, S.; Jenkins, S. J.; King, D. A. *J. Chem. Phys.* **2001**, *114*, 5765.
(78) Mittendorfer, F.; Hafner, J. *Surf. Sci.* **2001**, *472*, 133.
(79) Held, G.; Braun, W.; Steinruck, H. R.; Yamagishi, S.; Jenkins, S. J.; King, D. A. *Phys. Rev. Lett.* **2001**, *87*, 6102.
(80) Duschek, R.; Mittendorfer, F.; Blyth, R. I. R.; Netzer, F. P.; Hafner, J.; Ramsey, M. G. *Chem. Phys. Lett.* **2000**, *318*, 43.
(81) Lomas, J. R.; Pacchioni, G. *Surf. Sci.* **1996**, *365*, 297.
(82) Brizuela, G.; Castellani, N. *J. Mol. Catal. A: Chem.* **1999**, *139*, 209.
(83) Brizuela, G.; Castellani, N. *Surf. Sci.* **1998**, *401*, 297.
(84) Michaelides, A.; Hu, P. *J. Chem. Phys.* **2000**, *112*, 8120.
(85) Paul, J. F.; Sautet, P. *J. Phys. Chem. B* **1998**, *102*, 1578.
(86) Watwe, R. M.; Bengaard, H. S.; Rostrup-Nielsen, J. R.; Dumesic, J. A.; Norskov, J. K. *J. Catal.* **2000**, *189*, 16.
(87) Neurock, M.; van Santen, R. A. *J. Phys. Chem. B* **2000**, *104*, 11127.
(88) Pallassana, V.; Neurock, M. *J. Phys. Chem. B* **2000**, *104*, 9449.
(89) Horiuti, J.; Polanyi, M. *Trans. Faraday Soc.* **1934**, *30*, 1164.
(90) Farkas, A.; Farkas, L. *J. Am. Chem. Soc.* **1938**, *60*, 22.
(91) Te Velde, G.; Bickelhaupt, F. M.; Baerends, E. J.; Fonseca Guerra, C.; Van Gisbergen, S. J. A.; Snijders, J. G.; Ziegler, T. *J. Comput. Chem.* **2001**, *22*, 931.
(92) Vosko, S. H.; Wilk, L.; Nusair, M. *Can. J. Phys.* **1980**, *58*, 1200.
(93) Becke, A. D. *Phys. Rev. A* **1988**, *38*, 3098.
(94) Perdew, J. P. *Phys. Rev. B* **1986**, *33*, 8822.
(95) van Lenthe, E.; Baerends, E. J.; Snijders, J. G. *J. Chem. Phys.* **1993**, *99*, 4597.
(96) Somorjai, G. A. *Introduction to Surface Chemistry and Catalysis*; Wiley and Sons: New York, 1994.
(97) Deng, L. Q.; Ziegler, T. *Int. J. Quantum Chem.* **1994**, *52*, 731.
(98) Frisch, M. J.; Trucks, G. W.; Schlegel, H. B.; Scuseria, G. E.; Robb, M. A.; Cheeseman, J. R.; Zakrzewski, V. G.; Montgomery, J. A., Jr.; Stratmann, R. E.; Burant, J. C.; Dapprich, S.; Millam, J. M.; Daniels, A. D.; Kudin, K. N.; Strain, M. C.; Farkas, O.; Tomasi, J.; Barone, V.; Cossi, M.; Cammi, R.; Mennucci, B.; Pomelli, C.; Adamo, C.; Clifford, S.; Ochterski, J.; Petersson, G. A.; Ayala, P. Y.; Cui, Q.; Morokuma, K.; Malick, D. K.; Rabuck, A. D.; Raghavachari, K.; Foresman, J. B.; Cioslowski, J.; Ortiz, J. V.; Baboul, A. G.; Stefanov, B. B.; Liu, G.; Liashenko, A.; Piskorz, P.; Komaromi, I.; Gomperts, R.; Martin, R. L.; Fox, D. J.; Keith, T.; Al-Laham, M. A.; Peng, C. Y.; Nanayakkara, A.; Gonzalez, C.; Challacombe, M.; Gill, P. M. W.; Johnson, B.; Chen, W.; Wong, M. W.; Andres, J. L.; Gonzalez, C.; Head-Gordon, M.; Replogle, E. S.; Pople, J. A. *Gaussian 98*, Revision A.7; Gaussian, Inc.: Pittsburgh, PA, 1998.
(99) Montgomery, J. A.; Frisch, M. J.; Ochterski, J. W.; Petersson, G. A. *J. Chem. Phys.* **2000**, *112*, 6532.
(100) Curtiss, L. A.; Raghavachari, K.; Redfern, P. C.; Pople, J. A. *J. Chem. Phys.* **1997**, *106*, 1063.
(101) Saeys, M.; Reyniers, M.-F.; Marin, G. B.; Van Speybroeck, V.; Waroquier, M. *J. Phys. Chem. A*, submitted.
(102) Afeefy, H. Y.; Liebman, J. F.; Stein, S. E. Neutral Thermochemical Data. In *NIST Chemistry WebBook*, NIST Standard Reference Database Number 69; Linstrom, P. J., Mallard, W. G., Eds.; National Institute of Standards and Technology: Gaithersburg, MD, July 2001 (http://webbook.nist.gov).
(103) McQuarrie, D. A.; Simon, J. D. *Molecular Thermodynamics*; University Science Books: Sausalito, CA, 1999.
(104) Podkolzin, S. G.; Watwe, R. M.; Yan, Q.; de Pablo, J. J.; Dumesic, J. A. *J. Phys. Chem. B* **2001**, *105*, 8550.
(105) Watson, G. W.; Wells, R. P. K.; Willock, D. J.; Hutchings, G. J. *Chem. Commun.* **2000**, *8*, 705.
(106) Hammer, B.; Norskov, J. K. *Nature* **1995**, *376*, 238.
(107) Olsen, R. A.; Kroes, G. J.; Baerends, E. J. *J. Chem. Phys.* **1999**, *111*, 11155.
(108) Nobuhara, K.; Nakanishi, H.; Kasai, H.; Okiji, A. *Surf. Sci.* **2001**, *493*, 271.
(109) Neurock, M.; Pallassana, V. In *Transition State Modeling for Catalysis*; Truhlar, D. G., Morokuma, K., Eds.; ACS Symposium Series 721; American Chemical Society: Washington, DC, 1999.
(110) Clotet, A.; Pacchioni, G. *Surf. Sci.* **1996**, *346*, 91.